Observation of anisotropic diffusion of light in compacted granular porous materials

Alerstam, Erik; Svensson, Tomas

Published in:
Physical Review E (Statistical, Nonlinear, and Soft Matter Physics)

DOI:
10.1103/PhysRevE.85.040301

2012

PHYSICAL REVIEW E **85**, 040301(R) (2012)

Observation of anisotropic diffusion of light in compacted granular porous materials

Erik Alerstam[1,*] and Tomas Svensson[1,2,†]
[1]*Department of Physics, Lund University, P.O. Box 118, 221 00 Lund, Sweden*
[2]*European Laboratory for Non-linear Spectroscopy (LENS), 50019 Sesto Fiorentino, Italy*
(Received 25 January 2012; published 9 April 2012)

By analyzing spatio-temporal characteristics of short optical pulses diffusively transmitted through compacted granular materials, we reveal that powder compaction can give rise to strongly anisotropic light diffusion. Our disclosure represents a revision of the understanding of optics of powder compacts. Routes to material characterization and investigation of compression-induced structural anisotropy are opened, and the falsification of isotropic models have implications for quantitative spectroscopy of powder compacts (e.g., pharmaceutical tablets).

DOI: 10.1103/PhysRevE.85.040301 PACS number(s): 81.05.Rm, 42.25.Dd, 61.43.Gt, 78.55.Mb

The physics of granular media in general, and compression and deformation in particular, is utterly complex [1–4]. Material anisotropy due to compression is one phenomena in this context that remains poorly understood. It is known that uniaxial compression of certain granular media can induce anisotropy in mechanical properties [5,6], and scanning electron microscopy, pulsed-gradient stimulated-echo NMR, and spin-echo small-angle neutron scattering have recently confirmed that the pore structure itself indeed can be anisotropic [7–10]. The fundamental understanding of the interplay between compression, microstructure, and anisotropy is, however, still in its infancy [9]. In this Rapid Communication, we report that compression of granular matter also can give rise to anisotropic diffusion of light. Since the phenomenon is linked to pore space anisotropy, light scattering and diffuse spectroscopy may thus turn out to be a valuable, and nondestructive, tool for material characterization and for fundamental investigations of compression-induced anisotropy. As the materials in which we observe anisotropic light diffusion are of major technological importance, our findings also reveal an urgent need for better understanding of the microstructure and optics of compacted granular media. In particular, our results have implications for quantitative spectroscopy of, e.g., compacted powders and pharmaceutical tablets. Anisotropy can, for example, be a complication for spectroscopic methods that aim at separating the effects of scattering and absorption, methods which typically are based on isotropic diffusion models [11].

Anisotropic diffusion of light has been observed previously and studied in materials with a rather evident anisotropic microstructure, including etched porous semiconductors [12], nematic liquid crystals [13–16], fibrous and stretched plastics [17,18], wood [19], and biological tissues [20–22]. In contrast, we report on anisotropic diffusion in materials where the presence of microstructural anisotropy is far from self-evident and still the subject of active research, and where light propagation conventionally is assumed to be isotropic. In fact, the radial symmetry of the diffusion occurring in the compacted granular systems discussed here makes it impossible to detect optical anisotropy by looking for spatial asymmetries in reflected or transmitted steady-state intensity profiles. To reveal the anisotropic diffusion of light, we have instead relied on spatially resolved measurements of light transport dynamics. The main concept behind our approach is illustrated in Fig. 1.

The granular materials investigated are cylindrical compacts made by uniaxial compression of powders based on microcrystalline cellulose (MCC), lactose, or calcium phosphate. All samples have a diameter of 13 mm and a total weight of 500 mg. The compaction force applied varied between 5 and 55 kN, and thicknesses were between 1.9 and 3.5 mm. The MCC samples represent realistic pharmaceutical wet granulated compacts, and were manufactured from three different granule size fractions A, B, and C (granules being <150, 150–400, and >400 μm, respectively). Lactose and calcium phosphate samples were, on the other hand, made from pure powders (5–10 μm mean particle size). Additional details on the materials are found in the Supplemental Material [23]. For reference, we also make experiments on homogenous

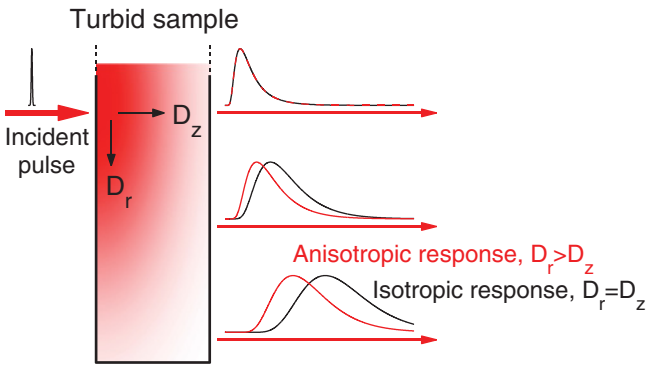

FIG. 1. (Color online) Measurement principle. In spatially resolved photon time-of-flight spectroscopy, anisotropic diffusion manifests itself as an anomalous spatial dependence of the arrival and shape of diffusively transmitted pulses. When radial diffusion is faster than longitudinal ($D_r > D_z$, in terms of diffusion constants), as in this study, pulses detected at nonzero radial positions arrive earlier and are narrower than what would be expected from analyzing on-axis transmission only, and then assume isotropic diffusion ($D_r = D_z$). In fact, the temporal shape of the pulse transmitted along the axis of incidence is independent of the radial diffusion constant.

*erik.alerstam@fysik.lth.se
†svensson@lens.unifi.it

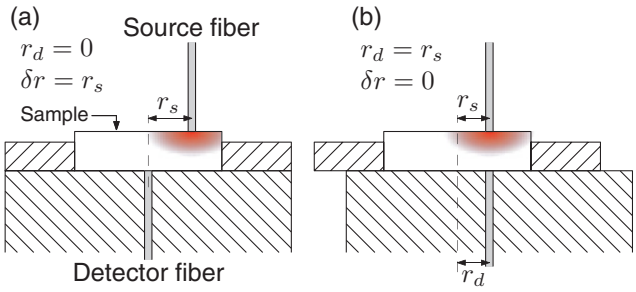

FIG. 2. (Color online) Experimental configuration. The detector fiber runs through the center of a cylindrical block. The sample is put on top, surrounded by a ring of having an inner diameter matching the sample. To reduce stray light, parts are made in black Delrin plastic. (a) shows the arrangement of spatially resolved PTOFS. Centering of the sample and ring sets $r_d = 0$. Sideways translation of the source fiber allows tuning of r_s. (b) shows how transverse translation of the sample and ring allows simultaneous tuning of r_d and r_s, a configuration used for the investigation of sample homogeneity (keeping $\delta r = 0$). When comparing with Fig. 1, note the rotated view.

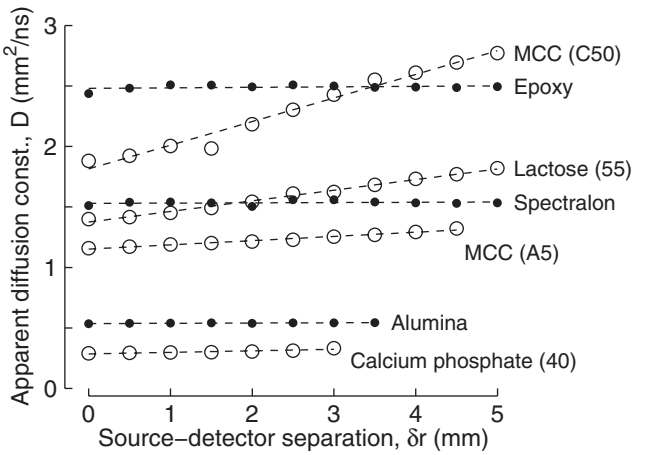

FIG. 3. The failure of isotropic modeling. For homogenous isotropic materials, isotropic diffusion modeling should result in the same fitted diffusion constant regardless of the source-detector separation used in the measurement. While this is the case for our isotropic reference materials (solid dots), it is evident that the compacted granular samples (open circles) cannot be modeled in the same manner. For clarity, the graph shows data only from a few of the samples (compression force in kN is given in parantheses).

isotropic turbid materials with scattering properties similar to those of the granular samples. These are Spectralon (a commercially available porous fluoropolymer), a macroporous sintered alumina ceramic [24,25], and a TiO_2-based epoxy phantom [26].

Light transport is investigated by conducting spatially resolved photon time-of-flight spectroscopy (PTOFS). Short (picosecond) pulses of 760-nm light are injected into the tablets at a radial position r_s using a 600-μm-core graded-index optical fiber, and light transmitted through the sample is detected at the radial positions r_d using a second identical fiber (radial positions defined relative to the sample center). A key parameter in measurements is the radial (transverse) source-detector separation, $\delta r = r_s - r_d$. The collected light consists of pulses that are temporally broadened due to multiple scattering, and the detection fiber directs these pulses to a fast photomultiplier that, combined with time-correlated single-photon counting, allows us to resolve them in time. Details on the spectroscopic instrument are available in Ref. [26], and the experimental configuration is elaborated in Fig. 2.

To avoid being very close to the edge of the samples (sample radii being 6.5 mm), measurements were conducted up to $\delta r = 5$ mm. For the most strongly scattering samples, however, there was an upper limit to δr above which the signal is so weak so that stray light distorts the obtained time-of-flight (TOF) histograms. In calcium phosphate samples and porous alumina, for example, light completely changes its direction on average each 5 μm (i.e., the transport mean free path of light is around 5 μm). The resulting high reflectivity and strong attenuation limits us to measurements up to δr of 3 mm. At larger δr, measurements are susceptible to stray light, e.g., light that exited the sample at lower δr and ideally should not reach the detector fiber. Analysis of the obtained photon TOF histograms are made by employing standard diffusion models generalized for anisotropic diffusion [14,15], and by using the extrapolated boundary conditions as described by Contini *et al*. [27] (additional details can be found in the Supplemental Material [23]).

The inadequacy of homogenous isotropic diffusion models is elucidated in Fig. 3. There, measurements at different source and detector separations are evaluated individually using the isotropic diffusion model (i.e., using the generalized diffusion model with $D_r = D_z$). If diffusion is isotropic, fitted diffusion constants should be constant (independent of δr). Data from the reference materials are thus in excellent agreement with isotropic diffusion, and show the capability of our system to deliver consistent data over a wide range of optical properties and source detector separations. At the same time, it is evident that the light transport in the compacted granular samples cannot be explained by homogenous isotropic diffusion. Note that also for the calcium phosphate data, although not easily seen in the figure, fitted diffusion constants are nonconstant and systematically increase with δr (growing from 0.29 mm^2/ns at $\delta r = 0$ to 0.33 mm^2/ns at $\delta r = 3$ mm).

One possible cause of the mismatch with the model of homogenous isotropic diffusion could, of course, be that our samples exhibit a spatially varying diffusion constant due to macroscopic density heterogeneity. However, careful investigation of the sample homogeneity ruled out this possibility. First, we investigated the radial sample homogeneity optically by making PTOFS measurements with $\delta r = 0$ at different positions of the samples [$r_s = r_d$ from 0 to 5 mm in steps of 0.5 mm; cf. Fig. 2(b)]. For the compacted granular samples, the coefficients of variation in fitted D were smaller than 3% (a similar variation was seen also for the isotropic reference materials), and the dependence on radial position was insignificant. This shows that our compacted samples are radially homogenous. To verify longitudinal homogeneity, our structures were also investigated by x-ray microtomography (μCT). Since radial homogeneity was confirmed by optical

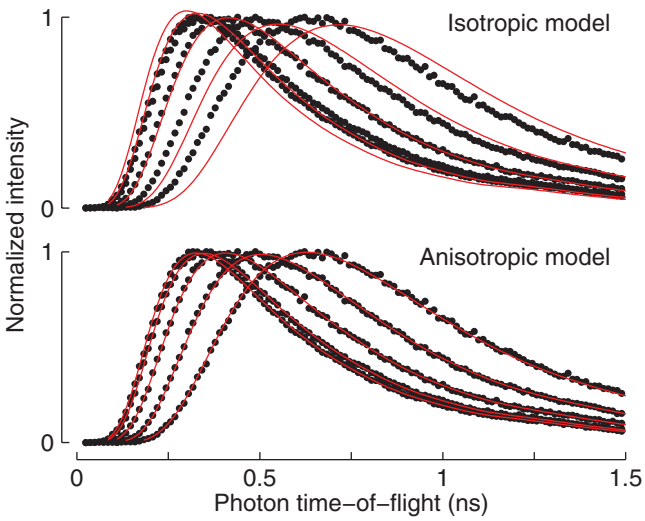

FIG. 4. (Color online) The spatio-temporal picture. When moving from isotropic to anisotropic modeling, fits (solid lines) obtained during the evaluation of spatially resolved PTOFS (i.e., simultaneous evaluation of all the spatial information in δr series) goes from being clear evidence of the model inadequacy to becoming virtually perfect. The displayed data (dots) are from the MCC C50 sample but are representative for all samples. For visual clarity, only a subset of the involved spatial recordings is shown ($\delta r = 0, 1, 2, 3, 4$ mm).

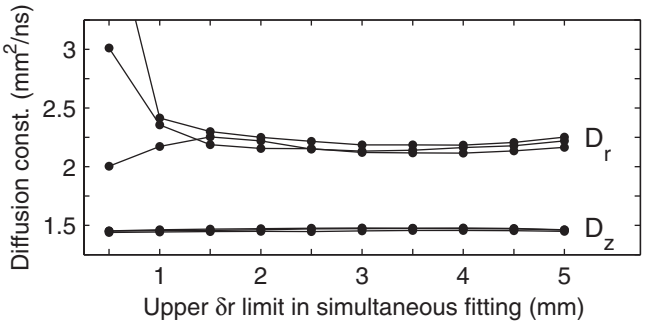

FIG. 5. The necessity of spatial information. Typical evolution of fitted radial and longitudinal diffusion coefficients (D_r and D_z) as increasingly more spatial information is included (i.e., evaluation involving all datasets up to an upper δr). In order to reach good estimates of both the longitudinal and radial diffusion constants, an evaluation must clearly include measurements made at δr being on the order of the sample thickness. Here, datapoints from three measurement repetitions from the MCC A (20-kN) sample are shown.

experiments, μCT scans were optimized for longitudinal density mapping. Still, there were no signs of heterogeneity.

Convincing evidence that anisotropy is the proper explanation for why homogenous isotropic diffusion modeling fails is presented in Fig. 4. There, simultaneous evaluation of the multiple TOF histograms of a δr series clearly shows that isotropic homogenous diffusion is far from being capable of explaining the experimental data, while the anisotropic diffusion model, with its two diffusion constants, results in excellent fits. Figure 4 gives only one example, but similar results were observed for all compressed granular samples. Even for the calcium phosphate samples, which, by looking at Fig. 3, may appear to be close to isotropic, a dramatic reduction of residuals is obtained when moving to anisotropic diffusion modeling. In comparison, and as expected, anisotropic modeling of data acquired from the isotropic reference materials results in an insignificant improvement of fits.

It is important to realize that the estimation of D_r requires measurements at $\delta r \neq 0$, while D_z can be estimated using only a single measurement at $\delta r = 0$. This can be inferred directly from anisotropic diffusion theory, and the issue is elaborated further in Fig. 5 by showing how estimates of diffusion constants evolve as the amount of spatial information increases. While the estimation of D_z is very robust, a proper evaluation of D_r requires the inclusion of measurements made at δr values comparable to the sample thickness. On the other hand, D_r converge to a constant value rather quickly. This means that inclusion of very large δr values is not necessary in general, making it possible to avoid low transmission measurements where stray light may distort data. Measurements made very close to the radial boundary may also be influenced by edge effects in material density, and eventually also by the breakdown of the infinite slab diffusion model. In fact, seen in Fig. 5, we generally observe a minor change in D_r when including measurements at high δr (when $\delta r = 5$ mm, the outer part of the fiber core is only 1.2 mm away from the sample boundary). In the following, our evaluation of anisotropy is therefore based on simultaneous evaluation of TOF histograms recorded at δr not larger than 4 mm (as mentioned earlier, the strongly scattering calcium phosphate samples are exceptions, and the evaluation is limited to δr not larger than 3 mm).

Figure 6 presents observed anisotropy factors $\gamma = D_r/D_z$ and longitudinal diffusion constants for all the materials. Measurement repetitions (also shown) show that the variation in derived D_z, D_r, and γ generally is very small. The coefficients of variation were between 0.3% and 3.3%, except for the 50-kN calcium phosphate, which gave a 6.6% percent variation in D_r and γ. The anisotropy of the MCC and lactose samples increases with pressure. Interestingly, this trend is not shared by the calcium phosphate samples. In this context, it is important to note also differences in the scattering properties. It is clear that the scattering strength is largely the same for the calcium phosphates. In contrast, scattering decreases with pressure for lactose and MCC samples (note, however, that a plateau is reached at 30 kN for MCC samples, after which scattering remains constant).

The fact that light propagation in compacted granular media can be strongly anisotropic represents a major revision of our understanding of the optics of such systems. It is therefore important to realize that our findings correlate well with recent reports on anisotropic pore structure. For example, pore space anisotropy of MCC compacts has been confirmed and has been shown to increase with compression force [8,10]. In addition, the pore space anisotropy reported in these studies occurs on length scales that should influence light scattering. The fact that radial diffusion is faster than longitudinal is presumably related to the formation of cracklike pores running perpendicular to the compression axis [7]. On the other hand, it should be noted that NMR porosimetry has been applied to, e.g., lactose and calcium phosphate samples without clear signs of anisotropy. However, the major difference in the way the pore

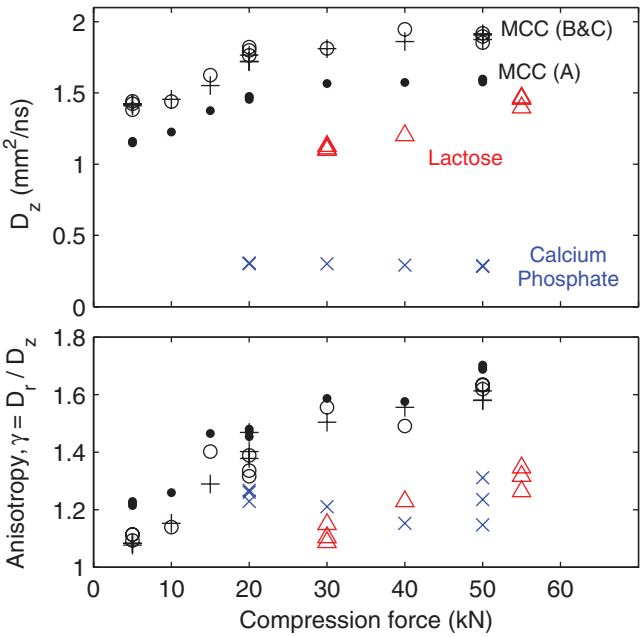

FIG. 6. (Color online) Anisotropy summary. Longitudinal diffusion constants and anisotropy factor $\gamma = D_r/D_z$ vs compression force for all samples. The general trend is that both anisotropy and diffusion constants increase with pressure (the increase in D corresponds to a decrease in scattering). MCC samples are shown as dots (•), plus signs (+), and circles (○), for the granule size classes A, B, and C, respectively. Lactose samples are given by triangles (△), and calcium phosphates by crosses (×). Note the three measurement repetitions for samples made at the lowest and highest compression force, as well as for the intermediate 20-kN MCC samples.

space is probed (and differences in samples) makes a deeper comparison meaningless. We note, instead, that anisotropy of *mechanical* properties has been observed for compacts based on all material investigated here [5,6], rendering our observations highly plausible. In fact, since light scattering and its wavelength dependence is extremely sensitive to microstructure, we believe that spectroscopic optical methods may turn out to be very useful and sensitive probes of pore space anisotropy. Conventional porosimetry methods such as mercury intrusion and gas adsorption do not give information about pore directionality, and currently employed methods that do are subject to important limitations [9].

Besides opening a route for the characterization of material anisotropy, our results also have obvious implications for quantitative spectroscopy of compacts in general. The use of isotropic diffusion models must be reconsidered. Moreover, considering a combination of anisotropic effects with density variations characteristic of more complex shapes of, e.g., pharmaceutical tablets [28], it is clear that model-based quantitative spectroscopy of powder compacts indeed is challenging. The picture gets even more complicated when considering also the more fundamental issue of how light samples complex porous structures [24,29].

To conclude, our observation of strong anisotropic diffusion of light in compacted granular media has broad implications. As discussed above, the phenomenon can be used for material characterization and fundamental investigations of compression physics, and also has important implications for quantitative spectroscopy of compacts. At the same time, reaching a full understanding of the relation between compression, microstructure, and light scattering is challenging, and this endeavor will require extensive and interdisciplinary efforts in the future.

This work was supported and generously funded by Stefan Andersson-Engels using grants from the Swedish Research Council. T.S. acknowledges support through a postdoctoral fellowship grant from the Swedish Research Council. Jonas Johansson is acknowledged for assisting in sample manufacturing, and Charles Mark Bee and the Imaging Technology Group at the Illinois Beckman Institute for conducting x-ray microtomography. We are also grateful to Diederik Wiersma for encouragement and for reading the manuscript.

[1] D. Train, J. Pharm. Pharmacol. **8**, 745 (1956).
[2] C. Goldenberg and I. Goldhirsch, Nature (London) **435**, 188 (2005).
[3] S. Luding, Nature (London) **435**, 159 (2005).
[4] C. C. Sun, J. Adhes. Sci. Technol. **25**, 483 (2011).
[5] T. Ando, H. Yuasa, Y. Kanaya, and K. Asahina, Chem. Pharm. Bull. **31**, 2045 (1983).
[6] M. P. Mullarney and B. C. Hancock, Int. J. Pharm. **314**, 9 (2006).
[7] Y. Wu, L. van Vliet, H. Frijlink, I. Stokroos, and K. van der Voort Maarschalk, Pharm. Sci. Technol. **9**, 528 (2008).
[8] V. Busignies, P. Porion, B. Leclerc, P. Evesque, and P. Tchoreloff, Eur. J. Pharm. Biopharm. **69**, 1160 (2008).
[9] R. Andersson, W. Bouwman, J. Plomp, F. Mulder, H. Schimmel, and I. De Schepper, Powder Technol. **189**, 6 (2009).
[10] P. Porion, V. Busignies, V. Mazel, B. Leclerc, P. Evesque, and P. Tchoreloff, Pharm. Res. **27**, 2221 (2010).
[11] Z. Q. Shi and C. A. Anderson, J. Pharm. Sci. **99**, 4766 (2010).
[12] P. M. Johnson, B. P. J. Bret, J. Gómez Rivas, J. J. Kelly, and A. Lagendijk, Phys. Rev. Lett. **89**, 243901 (2002).
[13] B. A. van Tiggelen, R. Maynard, and A. Heiderich, Phys. Rev. Lett. **77**, 639 (1996).
[14] D. S. Wiersma, A. Muzzi, M. Colocci, and R. Righini, Phys. Rev. Lett. **83**, 4321 (1999).
[15] D. S. Wiersma, A. Muzzi, M. Colocci, and R. Righini, Phys. Rev. E **62**, 6681 (2000).
[16] B. van Tiggelen and H. Stark, Rev. Mod. Phys. **72**, 1017 (2000).
[17] P. M. Johnson, S. Faez, and A. Lagendijk, Opt. Express **16**, 7435 (2008).
[18] P. M. Johnson and A. Lagendijk, J. Biomed. Opt. **14**, 054036 (2009).
[19] A. Kienle, C. D'Andrea, F. Foschum, P. Taroni, and A. Pifferi, Opt. Express **16**, 9895 (2008).
[20] A. Kienle, F. K. Forster, and R. Hibst, Opt. Lett. **29**, 2617 (2004).
[21] A. Kienle and R. Hibst, Phys. Rev. Lett. **97**, 018104 (2006).

[22] T. Binzoni, C. Courvoisier, R. Giust, G. Tribillon, T. Gharbi, J. C. Hebden, T. S. Leung, J. Roux, and D. T. Delpy, Phys. Med. Biol. **51**, N79 (2006).

[23] See Supplemental Material at http://link.aps.org/supplemental/10.1103/PhysRevE.85.040301 for some additional details.

[24] T. Svensson, E. Alerstam, J. Johansson, and S. Andersson-Engels, Opt. Lett. **35**, 1740 (2010).

[25] T. Svensson, E. Adolfsson, M. Lewander, C. T. Xu, and S. Svanberg, Phys. Rev. Lett. **107**, 143901 (2011).

[26] T. Svensson, E. Alerstam, D. Khoptyar, J. Johansson, S. Folestad, and S. Andersson-Engels, Rev. Sci. Instrum. **80**, 063105 (2009).

[27] D. Contini, F. Martelli, and G. Zaccanti, Appl. Opt. **36**, 4587 (1997).

[28] I. Sinka, S. Burch, J. Tweed, and J. Cunningham, Int. J. Pharm. **271**, 215 (2004).

[29] S. Faez, P. M. Johnson, and A. Lagendijk, Phys. Rev. Lett. **103**, 053903 (2009).